

# Pile-soil stress ratio in bidirectionally reinforced composite ground by considering soil arching effect

ZOU Xin-jun(邹新军)<sup>1</sup>, YANG Mei(杨眉)<sup>1</sup>, ZHAO Ming-hua(赵明华)<sup>1</sup>, YANG Xiao-li(杨小礼)<sup>2</sup>

(1. College of Civil Engineering, Hunan University, Changsha 410082, China;

2. School of Civil and Architectural Engineering, Central South University, Changsha 410075, China)

**Abstract:** To discuss the soil arching effect on the load transferring model and sharing ratios by the piles and inter-pile subsoil in the bidirectionally reinforced composite ground, the forming mechanism, mechanical behavior and its effect factors were discussed in detail. Then, the unified strength theory was introduced to set up the elastoplastic equilibrium differential equation of the subsoil under the limit equilibrium state. And from the equation, the solutions were derived with the corresponding formulas presented to calculate the earth pressure over and beneath the horizontal reinforced cushion or pillow, the stress of inter-pile subsoil and the pile-soil stress ratio. Based on the obtained solutions and measured data from an engineering project, the influence rules by the soil property parameters (i.e., the cohesion  $c$  and internal friction angle  $\varphi$ ) and pile spacing on the pile-soil stress ratio  $n$  were discussed respectively. The results show that to improve the load sharing ratio by the piles, the more effective means for filling materials with a larger value of  $\varphi$  is to increase the ratio of pile cap size to spacing, while to reduce the pile spacing properly and increase the value of cohesion  $c$  is advisable for those filling materials with a smaller value of  $\varphi$ .

**Key words:** composite ground; pile; geosynthetic-reinforced cushion; soil arching effect; pile-soil stress ratio

## 1 Introduction

Double direction or bidirectionally reinforced composite foundation (also named pile-net or pile-supported composite foundation) is an effective soft soil foundation treatment which has been developed in recent years. This kind of composite foundation is formed by setting a reinforced cushion (horizontal reinforcement which can adopt earthwork synthetic material, such as earthwork cloth, geotechnical grille and geocell) on the top of the reinforced pile (vertical reinforcement which can be flexible, semi-rigid or granular material pile). So it has the virtue of both the traditional vertical and the horizontal reinforcement technology<sup>[1-2]</sup>. And now it has been widely used at home and abroad<sup>[3-4]</sup>. HAN and GABR<sup>[4]</sup> made numerical analysis of the pile-net composite foundation. RAO and ZHAO<sup>[5]</sup> investigated the stress ratio of the pile-net composite foundation. CHEN et al<sup>[6]</sup> and XU et al<sup>[7]</sup> discussed the bearing mechanism of the geocell gravel cushion-gravel pile composite foundation and the pile-net composite foundation through indoor and outdoor model test separately. However, because of the complexity of interaction mechanism among pile, reinforced cushion and inter-pile soil, the theoretical study is still so little presently that it is far behind engineering practice.

Generally, the load transfer mechanism of this kind of composite foundation is composed by the soil arching effect, the film tension or the rigid beam slab effect of the reinforced cushion and the differential settlement effect led by the pile-soil relative stiffness. The degree of load transfer can be expressed by the stress ratio of pile to soil  $n$  ( $n = \sigma_c / \sigma_s$ ,  $\sigma_c$  is the stress on the pile top,  $\sigma_s$  is the stress of subsoil among piles). In this work, the influence of the soil arching effect on the stress ratio of pile and soil was mainly discussed.

Actually, TERZAGHI<sup>[8]</sup> discovered the soil arching effect during the model test. And he defined it as a phenomenon that stress was transferred from the yielded soil area to the unyielded soil area nearby. From then on, some researchers have conducted study in this field, such as the numerical analysis research of the soil arching effect by KOUTSABELOULIS and GRIFFITHS<sup>[9]</sup> and the analysis of soil arching forming process by HANDY<sup>[10]</sup>. And the engineering practice shows that the soil arching effect is beneficial to the stability of tunnel, retaining structure of slope or foundation pit. But the behavior of soil arching effect in bidirectionally reinforced composite foundation is quite different from that behind those familiar retaining structures. Little research work has been done on this type of soil arching effect at present, most of which is based on model test in the sandy filling. For example, LOW et al<sup>[11]</sup> examined

**Foundation item:** Project (07JJ4015) supported by the Natural Science Foundation of Hunan Province, China

**Received date:** 2008-09-05; **Accepted date:** 2008-10-18

**Corresponding author:** ZOU Xin-jun, PhD, Associate professor; Tel: +86-731-8821654; E-mail: xjzouhd@yahoo.com

the cylindrical soil arching effect aroused by sandy filler on the upper of the pile-beam by model test. HEWLETT and RANDOLPH<sup>[12]</sup> analyzed the spatial soil arching effect existing in the sandy filling of the embankment in foursquare pile layout based upon model test. While CHEN et al<sup>[13]</sup> further studied the three-dimensional soil arching effect in pile-supported embankments. However, the mechanism of soil arching effect is still not clear and worth performing deep study currently. And how to consider its favorable influence effect on the pile-soil stress ratio and bearing capacity of composite foundation has become the research focus and difficulty.

Therefore, a further discussion on the mechanism and the characteristic of the soil arching effect in bidirectionally reinforcement composite foundation was carried out by using the hemisphere model and the unified strength theory. And by setting the elastoplastic equilibrium equation of the foundation, the formulas were obtained to calculate the stress of pile top, the stress of soil among pile and the pile-soil stress ratio under rectangle pile layout, which may improve the calculation theory of composite foundation.

## 2 Mechanism of soil arching effect in bidirectionally reinforced composite foundation

For the soil arching effect in the embankment with the filling height  $H$  and unit weight  $\gamma$  of the filling, it is generally considered that the vertical earth pressure on the top of the soft soil foundation less than  $\gamma H$  indicates the soil arching effect, of which some typical models have been used, including prismatic, cylindrical and hemisphere, etc. And the prism model mostly uses the soil wedge shape advised by Carlson, which has been developed the Carlson soil wedge method. But this method considers that the filling load on top of the arch cone is all taken by pile top, which is obviously not consistent with the reality. So the hemisphere model is adopted in this work.

When the fill height exceeds the height of the pressure arch, the differential settlement between the top part of the soil piles and the soil on the top of the pile cap can make the stress of the embankment filling redistribute on the horizontal plane of the pile top within a certain range, and the major stress direction rotate to parallel with arch connection between two adjacent pile caps. Thus the compacted filling in this arch region forms an arch shell which transfers a part of the weight of the embankment on top of the soil between piles and pile cap (i.e., soil arching effect). The extent of this load transfer is relevant to properties of the filling, fill height, pile spacing and pile cap dimension, etc. If the pile spacing is too big, while the pile cap is too small, the soil

arching effect will be insufficient, which can make the soil between piles bear too much load, the differential settlement between the pile tops and the soils between piles exceeds the allowable range, the top surface of the embankment has a mushroom-shaped protuberance. In contrast, the due economic effect of the pile-supported embankment cannot be achieved.

According to HEWLETT's model experiment results<sup>[12]</sup>, the soil arch formed in the embankment filling above the pile top in foursquare pile layout is half-shell-shaped (Fig.1). In the further analysis of the single soil arch, one soil arch is split into two parts approximately, one is four triangular prism plane soil arches with two ends contacted with the top of the pile cap directly, and another is a sphere-shaped soil arch lapped on top of the four triangular prism plane soil arches (Fig.2). Part of the gravity above the soil between piles transferred to pile cap through soil arch makes the vertical stress of the pile cap greater than that of the soil between piles.

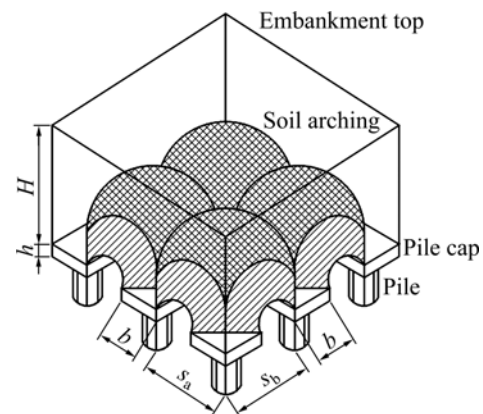


Fig.1 Soil arches in embankment

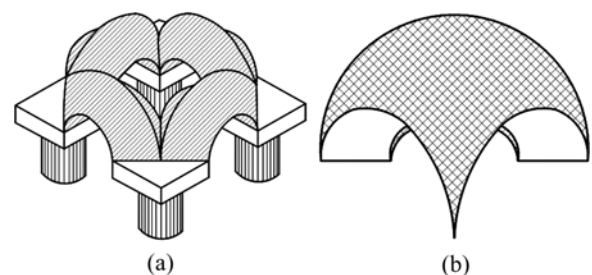


Fig.2 Uncoupling of single soil arch: (a) Four plane soil arch; (b) Sphere soil arch

Under the self-weight of the embankment, HEWLETT et al<sup>[12]</sup> considered that the plastic point of the soil arch must be located at the center point of the crown or the soil arch above the pile cap which cannot occur at other places. After a limit analysis of the elementary soil above the pile cap and that on the top of soil arch, he showed that:

$$\sigma_\theta = K_p \sigma_r \tag{1}$$

where  $\sigma_\theta$  and  $\sigma_r$  represent the tangential stress and radial stress of soil in polar coordinates, respectively; while  $K_p$  is the coefficient of Rankine's passive earth pressure.

Then two calculation formulas of the load sharing ratio were obtained. The smaller one in the two calculation results reflect that soil enters plastic state at this point, and the load sharing ratio by pile body was determined by this point, so the smaller value was chosen to be the practical load sharing ratio of pile body.

While CHEN et al<sup>[13]</sup> thought that when the embankment filling is too low (compared to pile spacing), neither the soil elements on the top of the pile cap, nor the soil elements on the top of the soil arch have entered limit state. Taking the soil elements on the top of the soil arch as an example, the resultant force of both pile-top earth pressures and inter-pile earth pressures calculated by using Eqn.(1) is greater than the gravity of the embankment. On the contrary, when the embankment filling is relatively high, the resultant force of both pile-top earth pressures and inter-pile earth pressures calculated under limit state is less than the gravity of the embankment. Only when the gravity of the embankment is a certain specific value (related to some factors such as pile spacing, pile cap dimension and properties of the filling), can the equilibrium condition of the embankment be met. Therefore, based on Eqn.(1), using undetermined coefficient  $\alpha$  ( $1/K_p \leq \alpha \leq 1$ ), i.e.,

$$\sigma_\theta = \alpha K_p \sigma_r \tag{2}$$

solving  $\alpha$  by the balance equation of embankment within the equivalent area for the single pile, the pile-soil load share ratio can be obtained.

The similarity between the two methods mentioned above is that they both start the research with balance equation of soil. Though they have considered the influence of part of the properties of the filling on the soil arching effect by the coefficient  $K_p$ , the consideration is not comprehensive, such as only containing the condition of foursquare pile layout while missing the influence of soil strength, cohesion, etc. Based on the unified strength theory, the formation conditions of the soil arching effect, the mechanical characters and the influencing factors of the soil arch in the quadrate pile layout were analyzed in this work.

### 3 Analysis model of soil arching effect in bidirectionally reinforced composite foundation

The hemisphere soil arch model in quadrate pile layout is shown in Fig.1. In Fig.1,  $H$  is the height of

embankment filling;  $s_a$  and  $s_b$  denote the pile spacing;  $b$  is the cap width, while  $h$  is the cap height. In this analysis, an assumption was made that the thicknesses throughout the soil arch is consistent, and adjacent soil arches don't overlap mutually. One soil arch is split into two parts approximately according to Fig.2. The force of the unit body on the top of the soil arch is shown in Fig.3 considering the influence of gravity (unit weight is  $\gamma$ ).

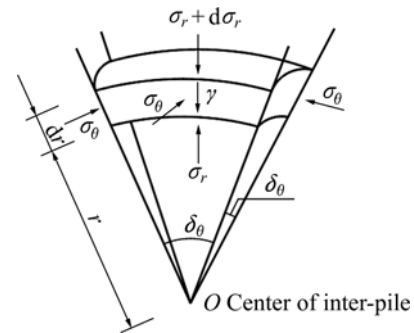


Fig.3 Analysis model of soil unit at top of arch

Based on Fig.3 and the equilibrium condition of micro-unit, the vertical balance equation of the unit on the top of the soil arch is

$$\frac{d\sigma_r}{dr} + \frac{2(\sigma_r - \sigma_\theta)}{r} = -\gamma \tag{3}$$

According to the symmetry of spherical coordinate system,  $\sigma_\theta = \sigma_\phi$  is obtained. And  $\sigma_\theta \geq \sigma_r$  is taken by earth pressure theory, accordingly  $\sigma_1 = \sigma_2 = \sigma_\theta = \sigma_\phi$ ,  $\sigma_3 = \sigma_r$ , and

$$\sigma_2 \geq (\sigma_1 + \sigma_3) / 2 - \sin \varphi (\sigma_1 - \sigma_3) / 2 \tag{4}$$

Thus it meets the unified strength theory<sup>[14]</sup>:

$$\left\{ \begin{aligned} F &= \frac{1 - \sin \varphi}{1 + \sin \varphi} \sigma_1 - \frac{b\sigma_2 + \sigma_3}{1 + b} = \frac{2c_0 \cos \varphi}{1 + \sin \varphi} \\ &(\sigma_2 \leq (\sigma_1 + \sigma_3) / 2 - \sin \varphi (\sigma_1 - \sigma_3) / 2) \\ F' &= \frac{1 - \sin \varphi}{(1 + b)(1 + \sin \varphi)} (b\sigma_2 + \sigma_1) - \sigma_3 = \frac{2c_0 \cos \varphi}{1 + \sin \varphi} \\ &(\sigma_2 \geq (\sigma_1 + \sigma_3) / 2 - \sin \varphi (\sigma_1 - \sigma_3) / 2) \end{aligned} \right. \tag{5}$$

According to the condition of the second formula (where  $c_0$  and  $\varphi$  are the cohesion and internal friction angle of the filling respectively), and  $\sigma_\theta$  in the second formula of Eqn.(5) can be calculated as

$$\sigma_\theta = \kappa \sigma_r + \frac{2c_0 \cos \varphi}{1 - \sin \varphi} \tag{6}$$

where  $\kappa = (1 + \sin \varphi) / (1 - \sin \varphi)$ .

Since Eqn.(6) is true only on condition that the soil has reached the limit state, it is set that

$$\sigma_\theta = \beta (\kappa \sigma_r + \frac{2c_0 \cos \varphi}{1 - \sin \varphi}) \tag{7}$$

where  $\beta$  is a undetermined coefficient,  $0 < \beta \leq 1$ .

And then, integrating Eqn.(3) and Eqn.(6), it can be obtained

$$\frac{d\sigma_r}{dr} + 2(1-\beta\kappa)\frac{\sigma_r}{r} - \frac{4\beta c_0 \cos \varphi}{r(1-\sin \varphi)} + \gamma = 0 \quad (8)$$

The solution to the equation above is

$$\sigma_r = Cr^{2(\beta\kappa-1)} - \frac{\gamma}{3-2\beta\kappa}r + \frac{2\beta c_0 \cos \varphi}{(1-\beta\kappa)(1-\sin \varphi)} \quad (9)$$

where  $C$  is the integral coefficient.

The pressure on the top of the soil arch  $\sigma_0$  (Fig.4) is the dead weight of the embankment filling above it.

$$\sigma_0 = \sigma_r \Big|_{r=\sqrt{s_b^2+s_a^2}/2} = \gamma(H - \sqrt{s_b^2+s_a^2}/2) \quad (10)$$

Taking Eqn.(10) as the boundary condition of Eqn.(9), the coefficient  $C$  may be obtained as

$$C = \left[ \gamma(H - \sqrt{s_b^2+s_a^2}/2) + \frac{\gamma\sqrt{s_b^2+s_a^2}}{2(3-2\beta\kappa)} - \frac{2\beta c_0 \cos \varphi}{(1-\beta\kappa)(1-\sin \varphi)} \right] / (\sqrt{s_b^2+s_a^2}/2)^{2(\beta\kappa-1)} \quad (11)$$

According to Eqn.(11) and Eqn.(9), taking  $r = \sqrt{(s_b-b)^2 + (s_a-b)^2}/2$ , we can obtain the pressure of the arch face under the top of the soil arch  $\sigma_{it}$ , then the stress on inter-pile subsoil  $\sigma_{su}$  may be educed as

$$\sigma_{su} = \sigma_{it} + \gamma\sqrt{(s_b-b)^2 + (s_a-b)^2}/2 \quad (12)$$

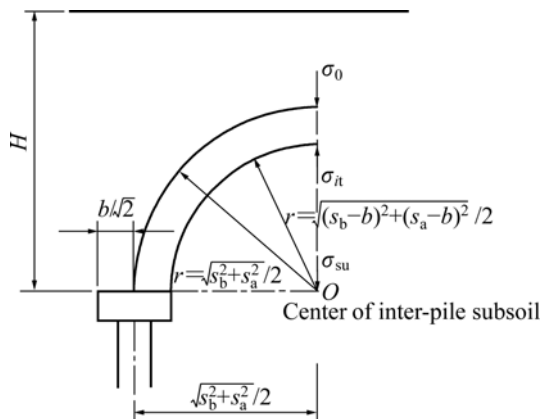


Fig.4 Analysis model of inter-pile subsoil

The soil arch above pile top consists of four plane arches. By the force analysis of soil elementary of pile top (Fig.5), the vertical balance equation was set as

$$\frac{d\sigma_r}{dr} + \frac{\sigma_r - \sigma_\theta}{r} = 0 \quad (13)$$

The relationship between the tangential stress and radial stress of the elementary soil of soil arch of pile top

is

$$\sigma_\theta = \beta_1 \left( \kappa\sigma_r + \frac{2c_0 \cos \varphi}{1-\sin \varphi} \right) \quad (14)$$

where  $\beta_1$  is the undetermined coefficient,  $0 < \beta_1 \leq 1$ , generally taking  $\beta = \beta_1$ .

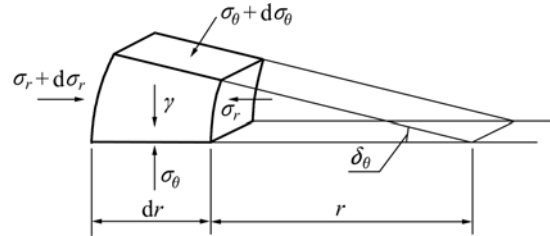


Fig.5 Stress analysis of soil unit above pile top

Then, integrating Eqn.(13) and Eqn.(14), it can be obtained

$$\sigma_r = Dr^{\beta\kappa-1} + \frac{2\beta c_0 \cos \varphi}{(1-\beta\kappa)(1-\sin \varphi)} \quad (15)$$

where  $D$  is the integral coefficient.

As shown in Fig.6, the pressure on the inside side of the soil arch of pile top is

$$\sigma_{ib} = \beta(\kappa\sigma_{su} + \frac{2c_0 \cos \varphi}{1-\sin \varphi}) \quad (16)$$

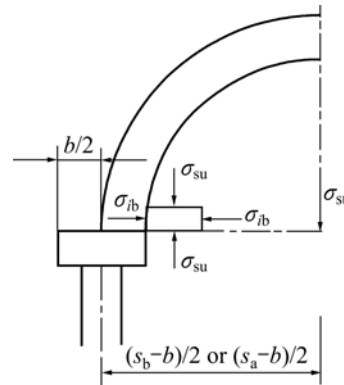


Fig.6 Inner stress analysis model of soil arch

Substituting  $\sigma_r \Big|_{r=(s_b-b)/2} = \sigma_{ib}$ ,  $\sigma_r \Big|_{r=(s_a-b)/2} = \sigma_{ib}$

in Eqn.(15), the integral coefficient of the plane soil arches in the long, short side may be attained as

$$\begin{cases} D_1 = (\sigma_{ib} - \frac{2\beta c_0 \cos \varphi}{(1-\beta\kappa)(1-\sin \varphi)}) / (\frac{s_b-b}{2})^{\beta\kappa-1} \\ D_2 = (\sigma_{ib} - \frac{2\beta c_0 \cos \varphi}{(1-\beta\kappa)(1-\sin \varphi)}) / (\frac{s_a-b}{2})^{\beta\kappa-1} \end{cases} \quad (17)$$

In order to calculate the load on the pile top shown in Fig.7, first the integral of the tangential stress of the

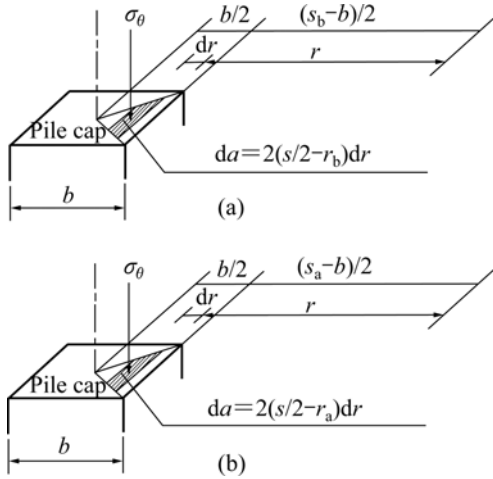


**Fig.7** Stress calculation model at pile top: (a) Long side; (b) Short side

soil on the pile top aroused by the plane soil arches in the long was calculated, short side respectively within the top of the pile cap, then the relevant pressure on pile top  $P_{u1}$  and  $P_{u2}$  may be attained, the sum of which is the pressure on pile top  $P_u$ :

$$\begin{cases} P_u = P_{u1} + P_{u2} \\ P_{u1} = 2 \int_{(s_b - b)/2}^{s_b/2} 2(s_b/2 - r)\sigma_\theta dr = E_1 + E_2 + E_3 + E_4 \\ P_{u2} = 2 \int_{(s_a - b)/2}^{s_a/2} 2(s_a/2 - r)\sigma_\theta dr = E_5 + E_6 + E_7 + E_8 \end{cases} \quad (18)$$

where

$$\begin{aligned} E_1 &= 2D_1 s_b \left[ \left(\frac{s_b}{2}\right)^{\beta\kappa} - \left(\frac{s_b - b}{2}\right)^{\beta\kappa} \right], \\ E_2 &= -\frac{4\beta\kappa D_1}{\beta\kappa + 1} \left[ \left(\frac{s_b}{2}\right)^{\beta\kappa + 1} - \left(\frac{s_b - b}{2}\right)^{\beta\kappa + 1} \right], \\ E_3 &= \frac{2s_b b c_0 \cos \varphi}{1 - \sin \varphi} \left[ \frac{\beta^2 \kappa}{1 - \beta\kappa} + \beta \right], \\ E_4 &= -\frac{4c_0 \cos \varphi}{1 - \sin \varphi} \left[ \frac{\beta^2 \kappa}{1 - \beta\kappa} + \beta \right] \left[ \left(\frac{s_b}{2}\right)^2 - \left(\frac{s_b - b}{2}\right)^2 \right], \\ E_5 &= 2D_2 s_a \left[ \left(\frac{s_a}{2}\right)^{\beta\kappa} - \left(\frac{s_a - b}{2}\right)^{\beta\kappa} \right], \\ E_6 &= -\frac{4\beta\kappa D_2}{\beta\kappa + 1} \left[ \left(\frac{s_a}{2}\right)^{\beta\kappa + 1} - \left(\frac{s_a - b}{2}\right)^{\beta\kappa + 1} \right], \\ E_7 &= \frac{2s_a b c_0 \cos \varphi}{1 - \sin \varphi} \left[ \frac{\beta^2 \kappa}{1 - \beta\kappa} + \beta \right], \\ E_8 &= -\frac{4c_0 \cos \varphi}{1 - \sin \varphi} \left[ \frac{\beta^2 \kappa}{1 - \beta\kappa} + \beta \right] \left[ \left(\frac{s_a}{2}\right)^2 - \left(\frac{s_a - b}{2}\right)^2 \right] \end{aligned}$$

For foursquare pile layout (i.e.  $s_b = s_a = s$ ),  $P_u = 2P_{u1}$ .

The undetermined coefficient  $\beta$  can be solved by the balance equation of the embankment within the equivalent area of a single pile, namely:

$$\gamma s_a s_b H = P_u(\beta) + \sigma_{su}(\beta)(s_a s_b - b^2) \quad (19)$$

If  $\beta < 1$ , it shows that the soil arch has not yet entered the plastic state, and the soil within the equivalent area of a single pile meets the equilibrium condition of forces. While if  $\beta = 1$ , the soil arch has just entered the plastic state. And if  $\beta > 1$ , it shows that the soil arch has entered the plastic state. When the soil arch enters the plastic state, the shared loading proportion cannot get further increase. So this part of unbalanced gravity should be distributed to pile cap and inter-pile subsoil by the load sharing ratio of pile when the soil arch has just entered the plastic state. This means after the soil arch has entered the plastic state, the load sharing ratio of pile keeps unchangeable, then  $\beta = 1$ . It also shows that the embankment has a critical height  $H_{cr}$  which makes the soil arch just enter the plastic state, namely  $\beta = 1$ . After obtaining  $\beta$  and  $P_u$ , the pile-soil stress ratio  $n$  and the load sharing ratio of pile  $E$  can be educed as

$$n = \begin{cases} P_u(\beta) / (s_a s_b \sigma_{su}), & \beta < 1 \\ P_u(l) / (s_a s_b \sigma_{su}), & \beta \geq 1 \end{cases} \quad (20)$$

$$E = \begin{cases} P_u(\beta) / (\gamma s^2 H), & \beta < 1 \\ P_u(l) / (\gamma s^2 H_{cr}), & \beta \geq 1 \end{cases} \quad (21)$$

If substitute  $\beta = 1$  into Eqn.(19), then the obtained  $H$  is just the critical height of embankment  $H_{cr}$ , which is related to the pile spacing, pile cap size and properties of the embankment filling. If let  $c_0 = 0$  and  $\beta = 1$ , then the solutions of Refs.[12–13] may be obtained, which can be seen as the special case of the method in this work.

#### 4 Application

One trial section project under treatment adopted prestressed pipe pile with an inner diameter  $d_1 = 220$  mm and external diameter  $d_2 = 400$  mm respectively<sup>[15]</sup>. The pipe pile was laid in foursquare with a pile spacing  $l = 2.4$  m. And a reinforced concrete support plate of  $100 \text{ cm} \times 100 \text{ cm} \times 35 \text{ cm}$  (thickness) was set above every pile top. After filling 30 cm-fine-sand on the top of the support plate, a layer of plastics-steel geotechnical grille was laid. The subsoil was silt and mucky sandy loam. Unit weight of the fill  $\gamma = 15 \text{ kN/m}^3$ . The filling height is 3.5 m. According to the result of indoor and outdoor tests,  $c = 10 \text{ kPa}$ ,  $\varphi = 30^\circ$ . The measured and calculated values of the stress of pile top, the stress of inter-pile subsoil and the pile-soil stress ratio above the geotechnical grille

cushion are listed in Table 1. The setting of earth pressure cell is shown in Fig.8.

**Table 1** Comparison of pile-soil stress ratio  $n$  above grille

Measured result			Calculated values		
$\sigma_c$ /kPa	$\sigma_s$ /kPa	$n$	$\sigma_c$ /kPa	$\sigma_s$ /kPa	$n$
167.35	4.37	38.28	225	10.83	20.7
167.35	17.9	9.35	225	10.83	20.7

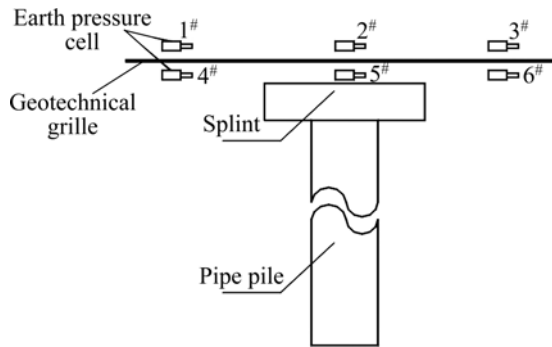


**Fig.8** Instrumented earth pressure cells around pile

From the comparison between the calculated and measured values, the calculated value of earth pressure on pile top above the grille is more than the observed result, while the calculated inter-pile subsoil stress value and the pile-soil stress ratio are among the observed values, which shows that the method in this work is consistent with the actual situation to some extent.

### 5 Parameters analysis

In order to discuss the influence rules by properties of subsoil, pile spacing, on the load sharing ratio of pile body, a parameter analysis was conducted in this work based on the engineering example above.

When analyzing the effect of pile spacing and other factors on the load sharing ratio of pile body  $E$ , the ratio  $\delta$  of the width of pile cap  $b$  to the pile spacing  $s$  was taken as 1/2, 1/3, 1/4 respectively, keeping other parameters constant. And then the changing curve of the load sharing ratio of pile body  $E$  versus the pile spacing was obtained as shown in Fig.9, which shows that the greater the value of  $\delta$ , the greater the load sharing ratio of pile body  $E$ . Especially within the familiar  $s/H$  range in engineering applications, the effect of  $\delta$  on the load sharing ratio of pile body  $E$  is much more obvious.

To analyze the effect of subsoil properties on the load sharing ratio of pile body  $E$ ,  $\phi$  was chosen as 20°, 30°, 40° respectively, while  $c$  changed within 0–30 kPa, keeping other parameters constant. Fig.10 shows that the

load sharing ratio of pile body  $E$  increases with the increasing  $c$  and  $\phi$ . In addition, it is shown in Fig.10 that within the familiar  $s/H$  range ( $0.3 \leq s/H \leq 0.6$ ) in engineering applications, adopting filling materials of greater internal friction angle in the range of embankment soil arch and properly increasing the cohesion value of the filling are beneficial to increasing the load sharing ratio of pile body  $E$ .

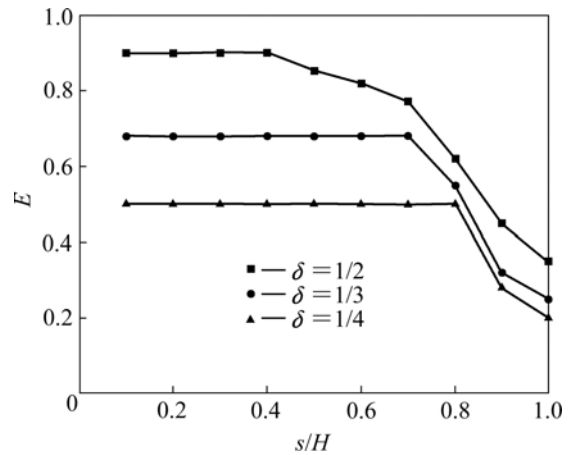


**Fig.9** Curves of load share( $E$ ) vs  $s/H$

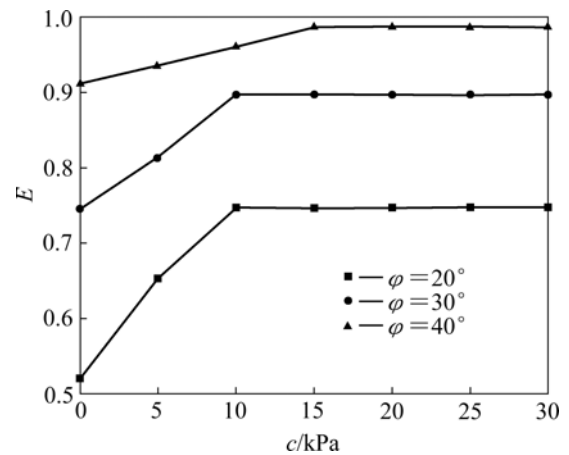


**Fig.10** Curves of load share( $E$ ) vs cohesion( $c$ )

### 6 Conclusions

1) The forming mechanism, mechanical behavior and affecting factors of the soil arching effect in the bidirectionally reinforcement composite foundation were analyzed in detail, and the hemisphere model was found reasonable to describe the soil arching.

2) By introducing the unified strength theory, the formulas to calculate the pile top stress, inter-pile subsoil stress and pile-soil stress ratio below or above the reinforced cushion were derived, application result of which shows a good agreement between the calculated values and measured data from an engineering example.

3) The parameters analysis based on the obtained

solutions shows that for filling materials with larger internal friction angle  $\varphi$ , under the condition that the bearing capacity and the deformation of single pile meet the requirements, increasing the ratio of pile cap width to pile spacing should be given the priority to improve the load sharing ratio by pile body  $E$ ; on the contrary, if the  $\varphi$  is smaller, the more effective means to increase  $E$  is to decrease the pile spacing and increase the cohesion( $c$ ).

## References

- [1] GONG Xiao-nan. The theory and application of the composite foundation[M]. Beijing: China Building Industry Press, 2002. (in Chinese)
- [2] ZHANG Ling, ZHAO Ming-hua, HE Wei. Working mechanism of two-direction reinforced composite foundation[J]. Journal of Central South University of Technology, 2007, 14(4): 589–594.
- [3] YAN Li, YANG Jun-sheng, HAN Jie. Geosynthetic-reinforced and pile-supported earth platform composite foundation[J]. Rock and Soil Mechanics, 2005, 26(5): 821–826. (in Chinese)
- [4] HAN J, GABR M A. Numerical analysis of geosynthetic-reinforced and pile-supported earth platforms over soft soil[J]. Journal of Geotechnical and Geoenvironmental Engineering, ASCE, 2002, 128(1): 44–53.
- [5] RAO Wei-guo, ZHAO Cheng-gang. The behavior of pile-net composite foundation[J]. China Civil Engineering Journal, 2002, 35(2): 74–80. (in Chinese)
- [6] CHEN Yan-ping, ZHAO Ming-hua, CHEN Chang-fu. Similarity model test of geocell reinforced gravel mattress and gravel pile composite foundation[J]. China Journal of Highway and Transport, 2006, 19(1): 17–22. (in Chinese)
- [7] XU Lin-rong, NIAN Jian-dong, LU Da-wei. Experimental study on pile-net composite foundation of high-speed railway on soft soils[J]. Rock and Soil Mechanics, 2007, 28(10): 2149–2154. (in Chinese)
- [8] TERZAGHI K. Theoretical soil mechanics[M]. New York: John Wiley and Sons, 1943: 66–76.
- [9] KOUTSABELOULIS N C, GRIFFITHS D V. Numerical modeling of the reape door problem[J]. Geotechnique, 1989, 39(1): 77–89.
- [10] HANDY L H. The arch in soil arching[J]. Journal of Geotechnical Engineering, ASCE, 1985, 111(3): 302–318.
- [11] LOW B K, TANG S K, CHOA V. Arching in piled embankments[J]. Journal of Geotechnical and Geoenvironmental Engineering, ASCE, 1993, 120(11): 1917–1938.
- [12] HEWLETT W J, RANDOLPH M F. Analysis of piled embankments[J]. Ground Engineering, 1988, 21(3): 12–18.
- [13] CHEN Yun-ming, JIA Ning, CHEN Ren-peng. Soil arch analysis of pile-supported embankments[J]. China Journal of Highway and Transport, 2004, 17(4): 1–6. (in Chinese)
- [14] YU M H. Unified strength theory and applications[M]. Berlin: Springer, 2001.
- [15] Guangdong Hangsheng Engineering Ltd. Report of soft subsoil section of the highway from Beijiao to Yuecong in Fusan[R]. Guangzhou: Guangdong Hangsheng Engineering Ltd, 2004. (in Chinese)

(Edited by LI Xiang-qun)